Analytica Chimica Acta 907 (2016) 45–53

Contents lists available at ScienceDirect

Analytica Chimica Acta

journal homepage: www.elsevier.com/locate/aca

Total phenol analysis of weakly supported water using a laccase-based microband biosensor

Alina N. Sekretaryova [a, c, *], Anton V. Volkov [b], Igor V. Zozoulenko [b], Anthony P.F. Turner [c], Mikhail Yu Vagin [a, b, **], Mats Eriksson [a]

[a] Division of Chemical and Optical Sensor Systems, Department of Physics, Chemistry and Biology, Linköping University, SE-581 83, Linköping, Sweden
[b] Laboratory of Organic Electronics, Department of Science and Technology, Linköping University, SE-601 74, Norrköping, Sweden
[c] Biosensors and Bioelectronics Centre, Department of Physics, Chemistry and Biology, Linköping University, SE-581 83, Linköping, Sweden

HIGHLIGHTS

- A novel screen printed microband array biosensor for *in situ* total phenol estimation in weakly supported media was developed.
- Numerical simulations using the finite element method with new periodic boundary conditions were performed.
- The use of the biosensor for tap water quality monitoring was demonstrated.
- The biosensor showed correlation with a standard method for total phenol analysis of wastewater samples.

GRAPHICAL ABSTRACT

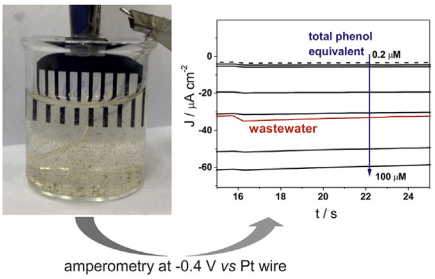

ARTICLE INFO

Article history:
Received 17 August 2015
Received in revised form
9 November 2015
Accepted 2 December 2015
Available online 19 December 2015

Keywords:
Laccase
Microelectrode
Microband
Electrochemical modeling
Total phenol analysis
Wastewater

ABSTRACT

The monitoring of phenolic compounds in wastewaters in a simple manner is of great importance for environmental control. Here, a novel screen printed laccase-based microband array for *in situ*, total phenol estimation in wastewaters and for water quality monitoring without additional sample pretreatment is presented. Numerical simulations using the finite element method were utilized for the characterization of micro-scale graphite electrodes. Anodization followed by covalent modification was used for the electrode functionalization with laccase. The functionalization efficiency and the electrochemical performance in direct and catechol-mediated oxygen reduction were studied at the microband laccase electrodes and compared with macro-scale electrode structures. The reduction of the dimensions of the enzyme biosensor, when used under optimized conditions, led to a significant improvement in its analytical characteristics. The elaborated microsensor showed fast responses towards catechol additions to tap water – a weakly supported medium – characterized by a linear range from 0.2 to 10 μM, a sensitivity of 1.35 ± 0.4 A M^{-1} cm^{-2} and a dynamic range up to 43 μM. This enhanced laccase-based

* Corresponding author. Division of Chemical and Optical Sensor Systems, Department of Physics, Chemistry and Biology, Linköping University, SE-581 83, Linköping, Sweden.
** Corresponding author. Division of Chemical and Optical Sensor Systems, Department of Physics, Chemistry and Biology, Linköping University, SE-581 83, Linköping, Sweden.
E-mail addresses: alina.sekretareva@liu.se (A.N. Sekretaryova), mikhail.vagin@liu.se (M.Y. Vagin).

http://dx.doi.org/10.1016/j.aca.2015.12.006

microsensor was used for water quality monitoring and its performance for total phenol analysis of wastewater samples from different stages of the cleaning process was compared to a standard method.

1. Introduction

Improving water resource management and increasing access to safe drinking water and basic sanitation are world-wide issues with the potential to improve the quality of life of billions of individuals [1]. The European Union Water Framework Directive, currently being implemented by all the Member states, addresses the management and protection of raw water supplies. This requires monitoring of both raw water and drinking water.

The monitoring of phenolic compounds in raw waters and wastewaters is of great importance for environmental control due to their wide use in industry and natural occurrence in various compounds [2]. The major anthropogenic sources of phenols are industrial waste from the pulp and paper, mineral and petroleum industries [3]. Many phenols are hazardous for humans, animals, plants and microorganisms and therefore the detection of low concentrations of phenols in water is an important issue [4]. Due to the high toxicity of phenols, there are many specific regulations regarding the phenol concentrations permitted in drinking and wastewaters. The European Council directives have set a limit of 0.5 μg L^{-1} for total phenol concentration in drinking water [5] and 0.1 mg L^{-1} for phenols in wastewater [4].

Various methods have been used for the determination of phenols in aqueous samples including traditional spectrophotometric methods [6] and high-performance liquid chromatography [7,8]. However, for rapid, specific and simple detection of phenolic compounds, biosensors present a more promising approach. A number of biosensors have been developed for phenol detection based on enzymes such as tyrosinase, peroxidase and laccase [9]. Laccase is used in the work presented here and is an enzyme containing copper at its active site, which catalyzes the reduction of molecular oxygen to water without the intermediate formation of hydrogen peroxide, thus simplifying the construction of a laccase-based biosensor [10]. Laccase has a broader substrate specificity than tyrosinase and peroxidase [11] and catalyzes the oxidation of various phenolic compounds, such as o-, p- and some m-diphenols, aminophenols, polyphenols, as well as phenol [12]. Laccase is therefore a candidate for total phenol measurements. A variety of biosensors for water sample analysis using laccase as a bio-recognition element have been reported recently [11,13–17]. (Table 1).

A general drawback of previously reported biosensors for phenol detection is their insufficient limits of quantification for phenols in water samples and the need for addition of electrolyte in the samples to enable the analysis. One way to improve the quantification limit and to overcome the need of additional electrolyte is by using microelectrodes, which exhibit a better signal/noise ratio than conventional-sized electrodes because they minimize the active surface area and the concomitant noise associated with the double layer capacitance, while enhancing mass transfer via multidimensional diffusion along directions where the electrode dimensions are small relative to the diffusion layer thickness [18]. However, immobilization of macromolecules such as enzymes on microelectrodes while retaining their catalytic activity is still a key challenge in the development of microelectrode-based biosensors [19]. There are only a couple of works in the literature on immobilization of laccase on microelectrodes. Kubota et *al*. [20] have investigated laccase immobilization on carbon-fiber microelectrodes (CFMEs, 10–20 fibers, 5 mm in length, 8 μm in diameter) via different immobilization techniques. The highest biosensor response was obtained using carbodiimide/glutaraldehyde for immobilization. The biosensor had a linear response to catechol between 1 and 90 μM with a sensitivity of 16 nA μM^{-1}. In another work [21], laccase was immobilized on CFMEs (7 μm in diameter and ca. 1.5 mm in length) by cross-linking of enzyme, bovine serum albumin and glutaraldehyde onto the single wall nanotube-modified CFMEs for the construction of a biofuel cell. However, the CFMEs utilized in both studies did not exhibit microelectrode behavior consistent with convergent mass transport, and thus are not suitable for analysis in electrolyte-free media. To the best of our knowledge, there is no previously reported work on a biosensor for phenol detection in weakly supported media without additional sample pretreatment, such as addition of electrolyte.

The microband design of microelectrodes [22] is a cost-effective and easily-fabricated compromise combining convergent mass transport, due to the microscale width as the critical dimension [23], and high output currents due to the macroscopic length. Among the various techniques available for microband electrode fabrication [24], screen printing stands out as an inexpensive approach [25]. The application of cross cutting [26–28] to deliver micro-scale thickness overcomes the problem of the insufficient resolution of screen printing in the lateral dimensions (approx. 50 μm).

In this study, we report on the development of a novel laccase-based microscale biosensor operating under a convergent diffusion regime. Screen printing followed by cross cutting was utilized for the fabrication of graphite microbands as a platform for further covalent immobilization of laccase. Numerical simulations utilizing the finite element method with a modified diffusion domain and new periodic boundary conditions developed for electrode arrays were used for modeling the voltammetric response of the developed microband electrodes. The diffusion domain approach is widely used for the simulation of microelectrode arrays [29–32]. Anodization followed by covalent modification via *N*-ethyl-*N*'-(3-dimethylaminopropyl)carbodiimide/N-hydroxysulfosuccinimide (EDC/NHS) chemistry was used for the electrode modification with laccase. Direct and mediated laccase bioelectrocatalytic oxidation of phenols was studied on macro- and microscale graphite electrodes. Significant enhancement of the analytical performance was achieved by the establishment of convergent diffusion at the microscale sensor which allowed, for the first time, the use of the developed amperometric biosensor for the direct analysis of weakly supported water samples without sample pretreatment. Finally, the developed microsensor was utilized to monitor phenolic compounds in wastewaters from different stages of the cleaning process.

2. Experimental

2.1. Reagents

All inorganic salts, N-hydroxysulfosuccinimide (NHS) sodium salt, 1-(3-dimethylaminopropyl)-3 ethylcarbodiimide (EDC), 1,1'-

Table 1
Analytical performance of different laccase based electrodes toward catechol.

Electrode description	Detection limit, μM	Dynamic range, μM	Sensitivity, A M^{-1} cm^{-2}	Storage stability	Water sample analyzed	Reference
Polydopamine/Lac-NiNPs/carbon nanofiber	0.69	1–910	0.025	30 days in 0.2 M acetate buffer (pH 5.5) at 4 °C	Tap water and lake water after filtration with membrane and 2-fold dilution with 0.2 M acetate buffer (pH 5.5)	[13]
Lac/reduced GO/chitosan/GCE	7	15–700	0.223	1 week in 0.1 M HAC–NaAC buffer solution (pH 4.5) at 4 °C	Tap water and lake water spiked with 0.5 and 1.0 mg mL^{-1} of hydroquinone in the HAC–NaAC buffer (pH 4.5)	[14]
Polyethyleneimine-AuNPs-Lac/GCE	0.03	0.36–11	–	90 days in air at 25 °C	Tap water, mineral and urban drainage water spiked with 0.8 μM of catechol were added to 0.1 M acetate buffer (pH 5.0)	[15]
Glutaraldehyde/Lac-NSTP/Au	0.05	0.1–100	0.0025	8 days in 0.05 M phosphate buffer at 4 °C	Olive oil mill wastewaters diluted with 0.1 M citrate buffer (pH 5.0)	[16]
Lac/SAM/Au	13	–	0.0115	One month in dry state at 4 °C	Surface water and industry wastewater 5-times diluted by 50 mM phosphate buffer (pH 6.5)	[11]
Lac-polyaniline/thick film interdigitated	–	0.2–1	–	–	Synthetic waste water diluted by 0.1 M acetate buffer (pH 4.5)	[17]
Lac/NHS-EDC/MBA	0.009	0.2–110	0.770	2 weeks in dry state at 4 °C, one month in 0.1 M acetate buffer (pH 5.0) at 4 °C	Tap and waste waters directly, without additional sample pretreatment	This work

Lac – laccase, NPs – nanoparticles, GO – graphene oxide, GCE – glassy carbon electrode, NSTP - N-succiniimidyl-3-thiopropionate, SAM – self-assembled monolayer.

ferrocenedimethanol, catechol and laccase from *Trametes versicolor* (activity ≥ 10 U mg^{-1}), were purchased from Sigma (Sweden). All chemicals were of reagent grade and used as received. Experiments were carried out with Milli-Q water from a Millipore Milli-Q system.

Waste water samples were obtained from the sewage treatment pilot plant at Hammarby Sjöstad (Sweden) and used as received.

2.2. Apparatus

The graphite microband arrays (MBA) were screen printed as described previously [25]. Briefly, carbon composite working electrodes were screen printed from graphite ink (7102 Carbon, DuPont) through a patterned stencil onto a polyethylene terephthalate (Hostaphane GN, Mitsubishi Polyester Film GmbH) plastic substrate. The printed structures were cured for 4 min at 130 °C, followed by screen printing of 5 layers of insulation ink (5018 A Dielectric, DuPont) on top of the graphite and then curing in UV (Aktiprint T). Arrays of 10 microbands with lengths of 0.6 and 0.8 mm, respectively, and 0.4 mm gap were fabricated (Fig. 1A). The graphite screen printed microband arrays were used as working electrodes after cutting normal to the substrate surface with office scissors. The microband working electrode was then connected to the potentiostat using a conductive adhesive tape and crocodile clips. An Autolab type III potentiostat system (Autolab, EcoChemie, Netherlands) was used for cyclic voltammetry (CV) and chronoamperometric measurements. The measurements were performed within a Faraday cage to reduce noise from surrounding equipment. It is possible, however, to use the microband electrode array without a Faraday cage as well for measurements in the field. Recovery of the microband electrode arrays was achieved by cutting a small portion of the working electrode in order to produce a new graphite surface.

A glassy carbon graphite disk electrode (GCE, diam. 3 mm, CH Instruments, Inc., USA) and a screen printed graphite disk electrode (SPD, diam. 4 mm, DropSens, Spain) were used as working electrodes of macroscopic dimensions. The GCE was successively polished with alumina powders (1.0 and 0.03 μm) followed by ultrasonication in pure water before use. An Ag/AgCl electrode in 3 M KCl, a saturated calomel electrode (SCE) (Radiometer, Copenhagen) or a platinum wire were used as reference electrode. A platinum wire was used as counter electrode.

GCE, SPD and MBA pretreatment was done by applying anodic potentials (ranging from +1.2 to +2.0 V) for 30 s in 0.05 M phosphate buffer solution (pH 7.0) [33]. In addition GCE pretreatment was also done by a 5 min potential pulse at 1.8 V followed by a 1 min potential pulse at −1.5 V in 0.05 M phosphate buffer solution (pH 7.0) [34].

2.3. Assessment of the surface concentration of carboxylic groups

The toluidine blue (TB) method [30,35] was utilized for the estimation of the amount of carboxylic groups on the electrode surfaces. Pretreated electrodes were soaked in 0.5 mM TB in 0.1 mM NaOH overnight for TB binding. Then the electrode surface was washed with 0.1 mM NaOH solution and pure water twice. The amount of TB molecules attached to the electrode surface was estimated by optical and electrochemical measurements assuming 1:1 stoichiometry of the TB-carboxylic group complex.

In the optical protocol, 100 μL of 50% acetic acid was added to remove the TB dye from the carboxyl groups on the surface of the electrode. The optical density of the solution was measured at 630 nm using a microplate reader. The concentration of released TB was determined using a calibration plot. For the electrochemical protocol, a scan rate study of the voltammetric response of the TB-modified electrodes allowed an estimation of the surface coverage [36].

2.4. Laccase activity assay

One unit of laccase activity was defined as the amount of enzyme oxidizing 1 μmol substrate per minute. Suitable amounts of enzyme necessary to obtain an absorbance of 0.4–1.0 after approximately 1.5 min was used in all photometric measurements. The ABTS (ε_{420} = 36000 M^{-1} cm^{-1}) test was performed in 100 mM acetate buffer at pH 5.0 with 0.8 mM final concentration of the substrate [37]. The laccase activity was found to be 10.5 ± 0.4 U mg^{-1}.

2.5. Laccase immobilization

Enzyme immobilization onto the electrode surface was done via EDC/NHS coupling between amine groups of laccase and the carboxylic groups of the pretreated electrodes [38]. The GCE, SPD or MBA electrodes were left in 5 mM NHS and 5 mM EDC solution in water for 2 h at room temperature for surface modification. After rinsing with distilled water, the electrodes were left in a laccase solution in water (100 U mL^{-1}) at 4 °C overnight. The non-

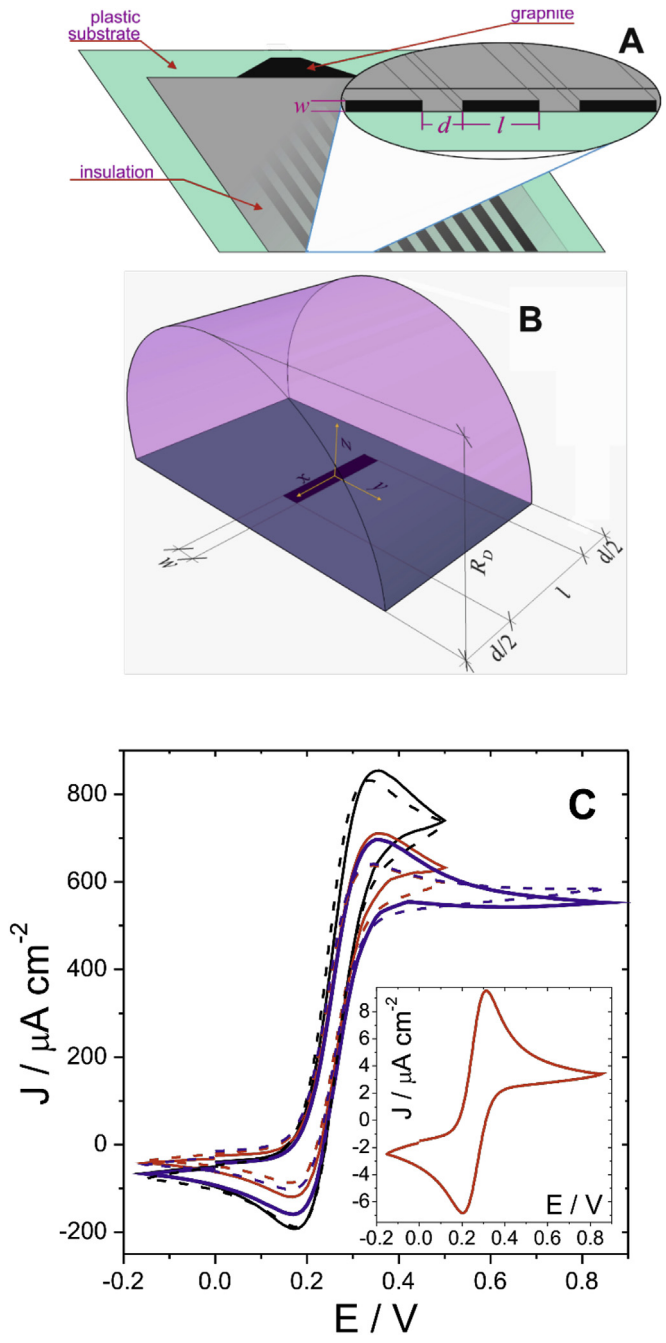

Fig. 1. Microband electrode characterization. **A**: The layout of the screen printed graphite microband electrode arrays; **B**: Simulation domain at a single microband electrode; **C**: Experimental and simulated voltammetric responses (solid and dashed curves, respectively) of ferrocenedimethanol at the graphite microband electrode (0.1 M HCl, 1 mM FcDM, scan rates: 50 mV/s (red and blue curves) and 200 mV/s (black curves); Inset: voltammetric response at the graphite disk electrode.

immobilized enzyme was removed by repeated washing with deionized water. The laccase-modified electrodes were stored at 4 °C in 0.1 M acetate buffer solution (pH 5.0) when not in use. The fabrication time for the MBA-based biosensor was minimum 10 h.

2.6. Real sample analysis

As a reference method for phenols detection, gas chromatography–mass spectrometry tandem mass spectrometry (GC–MS/MS) (triple quadrupole) in electron impact mode and multi reaction monitoring was used. The GC instrument was an Agilent Technology 7890 A connected to an Agilent 7000 A mass spectrometer and an Agilent 7683B autoinjector. The water samples were concentrated in a solid phase column at pH 2 prior to measurements. The sample was eluted from the column with organic solvents. The eluate was dried over sodium sulfate before derivatization with N-Methyl-N- (trimethylsilyl) trifluoroacetamide. The derivatized sample was analyzed by GC–MS/MS.

For electrochemical measurements a platinum wire was used for analysis of water samples as a pseudo-reference electrode instead of separate counter and reference electrodes. The applied potential used for amperometric measurements was −0.4 V (*vs* the Pt wire), which corresponds to 0 V *vs* the SCE. A Faradaic cage was used for the real sample analysis. This was, however, only necessary in order to substantiate the performance, while in field analysis high enough signal-to-noise ratios can be achieved by the developed microband electrodes.

3. Theoretical model of the microband electrodes

A rectangular form of each microband electrode in the array (Fig. 1A) was assumed with a microband width w of 7 μm [25], a length l of 0.4 mm and a distance between the electrodes in the array d of 0.4 mm. In order to describe the voltammetric response of the MBA, a single electrolyte domain (Fig. 1B) bound to a single graphite microelectrode and the surrounding in-plane insulator were chosen.

Both species A and B involved in mass transport undergo a one-electron redox reaction at the electrode surface:

$$A \underset{k_b}{\overset{k_f}{\rightleftarrows}} B + e^- \tag{1}$$

where k_f and k_b are the forward and backward rate constants. Only species A is present in the bulk solution. If the electrode reaction follows Butler-Volmer kinetics, the rate constants can be defined as:

$$k_f = k^\circ \exp\left\{\frac{(1-\alpha)F(E(t)-E^\circ)}{RT}\right\},\ k_b = k^\circ \exp\left\{\frac{-\alpha F(E(t)-E^\circ)}{RT}\right\} \tag{2}$$

where k° is the standard electron transfer rate constant, α=0.5 is the transfer coefficient, F is the Faraday constant, E° is the formal potential of the redox couple, $E(t)$ is the potential applied to the microband electrode, R is the gas constant and T (298 K) is the temperature.

The mass transport of species in Cartesian coordinates is described by Fick's second law of diffusion:

$$\frac{\partial c_A}{\partial t} = \vec{\nabla}(D_A \vec{\nabla} c_A)$$
$$\frac{\partial c_B}{\partial t} = \vec{\nabla}(D_B \vec{\nabla} c_B) \tag{3}$$

where D_A and D_B are the diffusion coefficients, c_A and c_B are the concentrations of the species, respectively.

The boundary condition for eq. (3) at the electrode surface $\left(z = 0, -\frac{l}{2} \le x \le \frac{l}{2}, -\frac{w}{2} \le y \le \frac{w}{2}\right)$ is given by:

$$-D_A \vec{n} \vec{\nabla} c_A = D_B \vec{n} \vec{\nabla} c_B = k_f c_A - k_b c_B \tag{4}$$

where $\vec{n}$ is a normal vector. Zero normal flux at the bottom

insulator boundary has been assumed:

$$-D_A \vec{n} \vec{\nabla} c_A = -D_B \vec{n} \vec{\nabla} c_B = 0 \quad (5)$$

A constant bulk concentration (c_A=1 mM, c_B=0 M) has been assumed on the top surface of the domain ($y^2 + z^2 = R_D^2$, $z > 0$). The initial concentrations in the computational domain are assumed to be constant and equal to the bulk concentration. Here, $R_D = 6\sqrt{2t_0 D_A}$ is the maximum extent of the diffusion layer over the duration of the simulation. A periodic boundary condition has been set along the x direction in order to take into account the periodic structure of the microband array:

$$\begin{aligned} c_A|_{x=\frac{l}{2}+\frac{d}{2}} &= c_A|_{x=-\left(\frac{l}{2}+\frac{d}{2}\right)} \\ D_A \vec{\nabla} c_A|_{x=\frac{l}{2}+\frac{d}{2}} &= D_A \vec{\nabla} c_A|_{x=-\left(\frac{l}{2}+\frac{d}{2}\right)} \\ c_B|_{x=\frac{l}{2}+\frac{d}{2}} &= c_B|_{x=-\left(\frac{l}{2}+\frac{d}{2}\right)} \\ D_B \vec{\nabla} c_B|_{x=\frac{l}{2}+\frac{d}{2}} &= D_B \vec{\nabla} c_B|_{x=-\left(\frac{l}{2}+\frac{d}{2}\right)} \end{aligned} \quad (6)$$

In the CV simulation the electrode surface potential is imposed to vary back and forth between two potentials with constant scan rate (Supplementary Note 1). The simulation was performed using the COMSOL Multiphysics 4.3b software provided by the Swedish National Infrastructure for Computing (SNIC) at Linköping University. Eq. (3) with its accompanying boundary conditions eqs. (4)–(6) was solved using the Transport of Diluted Species interface. The computation domain was meshed using a free triangular mesh. Different sizes of the mesh elements were tested to ensure the accuracy of the simulation. In order to solve the problem accurately, the direct MUMPS solver was used.

The average current density for the MBA is assumed to be equal to the current density for a single microelectrode. Thus, the average current density could be obtained by surface integration over the electrode boundary:

$$j = -\frac{F}{wl} \int_{-\frac{l}{2}}^{\frac{l}{2}} \int_{-\frac{w}{2}}^{\frac{w}{2}} D_A \vec{n} \vec{\nabla} c_A|_{z=0} dxdy \quad (7)$$

4. Results and discussion

4.1. Microband electrode array characterization

One of the possible approaches to achieve performance enhancement of an electroanalytical system, such as improved detection limit and increase in sensitivity, is the modification of the working electrode design to facilitate convergent mass transport. Shrinkage of the electrode dimensions improves the detection limit due to an increase of the Faradaic to capacitive current ratio [39,40]. Voltammetric responses of the ferrocenedimetanol redox probe ($D_A = D_B = 7 \times 10^{-6}$ cm^2/s , $k^\circ = 2 \times 10^{-2}$ cm/s, E°= 0.255 V) were studied on the graphite screen printed electrodes (Fig. 1C). The MBA showed pronounced sigmoidal voltammetric responses, typical for micro-scale electrodes with enhanced mass transport of the redox material to/from the electrode, due to convergent diffusion. The transition from redox peak currents obtained at the macro-scale electrode (Inset of Fig. 1C) to the wave-shaped response of the micro-scale electrode, is due to the enhancement of rates of reactant and product mass transfer to and from the electrode surface respectively [41], as a result of convergent diffusion. Assuming a microband electrode width of 7 μm [25], more than two orders of magnitude larger current density for the redox process was obtained with the micro-scale electrode, which illustrates the sensitivity increase achieved due to convergent diffusion. The enhancement of the sensitivity at the MBA was larger than obtained for charged redox probes (ferro/ferricyanide and hexaaminerruthenium) [25], which probably illustrates the different contributions of surface states to the electrode reaction kinetics. The observed voltammetric responses on the MBA were still characterized by peak redox currents and a dependence of the currents on the scan rate. This illustrates that the observed current plateaus are not true steady-state currents. Thus, although having enhanced mass transfer, leading to a current density increase, the microband arrays showed mixed diffusional behavior over the time domain of the recorded cyclic voltammograms.

The experimental data collected at different scan rates and anodic limits showed good agreement with simulated voltammetric responses obtained with the use of the new model developed for the MBA. The small difference between numerical and experimental data could be related to uncertainty in the estimated values of diffusion coefficient, geometrical parameters of the device and the initial bulk concentrations. One or a few of these parameters could be varied to fit the experimental data. The concentration profiles of the reactant species (Fig. A.2) obtained at potentials of steady-state and zero currents, show highly nonlinear diffusion, which spreads mostly in the radial direction. Since the distance between the microelectrodes is large, a small overlapping between the diffusion clouds is observed only at high scan rates.

Being the critical dimension of the microscale electrode [23], the microband electrode width limits the observed current density. In accordance with our previous findings [25], the modelling revealed only a minor influence of the distance between the microelectrodes and the microband length on the values of the observed current densities, laying within the error of the utilized method of numerical simulations (data not shown).

The theoretical modelling thus confirms that the rather crudely produced microbands, in particular the cross cutting with scissors, do indeed show the expected microband electrode behavior. The modelling furthermore allows for further electrode development and a better understanding of the three dimensional reactant concentrations.

4.2. Electrode pretreatment for covalent laccase immobilization

Different immobilization techniques [20,42,43] and various electrode materials and configurations [44–46] have previously been used in the construction of biosensors for phenol detection. Covalent enzyme immobilization via EDC/NHS chemistry [38] was chosen for laccase attachment to the electrode surface due to the fast and easy protocol [20] and the resulting enzyme stabilization.

Carboxylic groups, required for binding the enzyme via EDC/NHS, were introduced onto the surface of the GCE, SPD and MBA by anodization at various anodic potentials and quantified by two electrochemical methods, differential pulse voltammetry (DPV) [33,34] and TB detection [35].

DPV (Fig. A.3) revealed the presence of a distinct redox peak at potentials −0.1 V – +0.1 V depending on electrode surface, assigned to the carboxylic functional groups [47], appearing after the pretreatment. The pretreatment of GCE at different potentials during a short time (30 s) did not lead to any peak appearance. However, pretreatment by a 5 min potential pulse at 1.8 V followed by a 1 min potential pulse at −1.5 V [34] led to the appearance of a

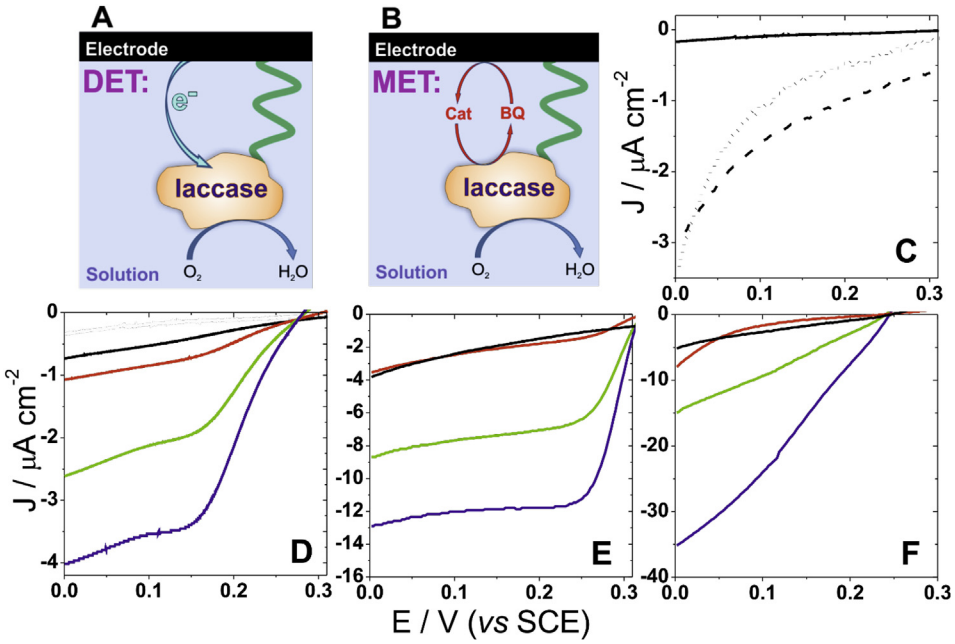

Fig. 2. Bioelectrocatalysis on laccase-modified carbon electrodes. **A** and **B** represent the schemes of direct electron transfer (DET) and mediated electron transfer (MET), respectively, Cat and BQ are catechol and benzoquinone, respectively. **C**: DET on laccase-modified electrodes. Background-subtracted linear sweep voltammograms obtained at laccase-modified GCE, SPD and MBA (solid, dotted and dashed curves, respectively) in air-saturated buffer. **D**, **E** and **F**: MET on laccase-modified GCE, SPD and MBA respectively. Linear sweep voltammograms obtained after addition of 0, 10, 50 and 100 μM (black, red, green and blue curves, respectively) of catechol; 0.1 M acetate buffer, the scan rate is 1 mV s^{-1}.

well-defined response of the oxygen functional groups. In contrast to the SPD (Fig. A.3B), the MBA showed the presence of a characteristic peak even before anodization (Fig. A.3C), which indicates the creation of carboxylic groups and mechanical activation of the graphite surface by the cutting. Increase of the anodization potential of the MBA led to the redox peak rising and accordingly higher activation of the graphite surface. A growth of the background currents with increase of the anodization potential, as a result of a surface area increase, was seen for all electrode structures. The GCE responses were characterized by more than one order of magnitude larger background currents. These effects illustrate the different surface properties of the studied electrode structures.

The quantification of the TB molecules bound to the activated surface, assuming a 1:1 stoichiometry for the assessment of the surface concentration of the carboxylic groups, was carried out independently by spectroscopy [30,35] and by electrochemistry (Supplementary Note 2). The surface concentrations of the carboxylic groups on the SPD and the GCE quantified by spectroscopy and electrochemistry are in a good agreement (Table A.1). Moreover, the height of the DPV redox peaks, assigned to carboxylic functionality, correlates well with the carboxylic group surface concentrations assessed via the TB method.

Anodization of the microband under optimized conditions as indicated by the DPV measurements, showed a larger total concentration of immobilized TB compared to the other anodization conditions of the MBA and to the other electrodes. The optimized conditions of anodization for all three electrode materials were used in the further studies.

4.3. Properties of the laccase-modified electrodes

The carboxylic groups created on the electrode surface by anodization were used for covalent immobilization of laccase via EDC/NHS chemistry [38]. Laccases can undergo both direct and mediated heterogeneous electron transfer between the electrode surface and the active site of the enzyme (Fig. 2A and B) [48]. Being immobilized onto the electrode surface, laccases catalyze four-electron oxygen reduction to water via direct electron transfer [10], appearing as an increase of the cathodic current of oxygen reduction in the presence of the enzyme (Fig. 2C). In spite of a higher surface concentration of carboxylic groups available for enzyme immobilization, the GCE showed smaller catalytic current densities in comparison with both screen printed electrode structures, which probably relates to the presence of graphite particles in the printed graphite ink, which can enhance the direct electron transfer efficiency [33].

The presence of organic substrate molecules, e.g. catechol, which can be re-reduced at the electrode surface and act as an electron shuttle between the active site of laccase as an oxidizer and the electrode surface as a reducer, leads to the concept of mediated electron transfer manifested as an increase in the cathodic current of oxygen reduction (Figs. 2D–3F) [10].

It should be stressed that true mediated bioelectrocatalysis of laccases should appear as an increase in the reduction current with increased substrate concentration due to the laccase-catalyzed substrate oxidation by oxygen at potentials close to 0 V (*vs* SCE). The contradictious data commonly found in recent literature and characterized by an increase in anodic current upon substrate concentration increase, only testifies to the oxidation of the substrate at the modified electrode surface, which makes those observations irrelevant to mediated laccase bioelectrocatalysis.

Amperometry was utilized for measurements using the laccase-modified microscale electrodes under optimized conditions. The catalytic current output was directly proportional to the substrate concentration. A pH study (Fig. A.5A) showed a maximum amperometric response for 10 μM catechol at pH 5.0, which is in agreement with previously reported values for *T. versicolor* laccase immobilized via EDC/NHS chemistry [16]. A potential study (Fig. A.5B) showed maximum response for 10 μM catechol at 0 V (*vs* SCE), and this is also similar to values reported previously [16] and

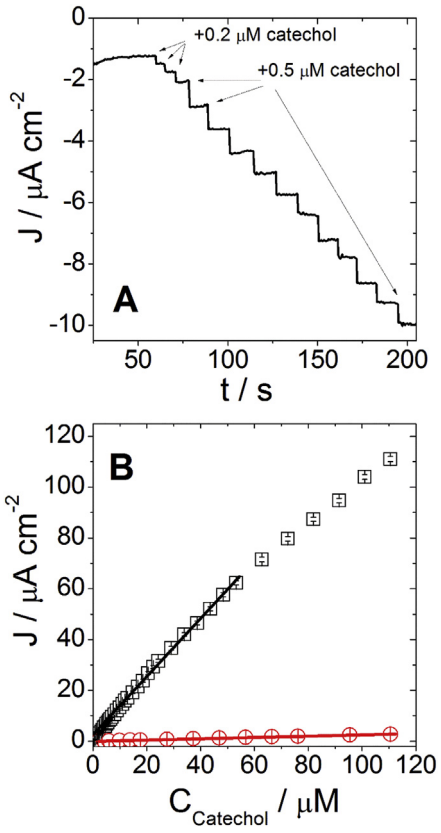

Fig. 3. Enhanced analytical performance of the laccase-modified MBA. **A**: An example of amperometric response of the laccase-modified MBA to successive additions of catechol solution at 0 V potential *vs* SCE (0.1 M acetate buffer); **B**: Calibration curves for the laccase-modified MBA (□) and the SPD (○) (P = 0.95, n = 5, error bars represent the standard deviation of a t-student distribution).

minimizes the possible interference by other compounds present in water samples.

The amperometric response of the MBA modified with covalently attached laccase (for a comparison with MBA electrodes modified with adsorbed enzyme see Fig. A.6) upon addition of catechol under optimized conditions (Fig. 3A) showed an excellent operational stability, which reflects a balanced mass transfer of reagent and product to/from the electrode surface. The calibration plots obtained for both laccase-modified SPD and MBA (Fig. 3B) reflect a significant improvement in the analytical performance for the MBA. A significant decrease in the limit of detection (from 0.8 μM for the SPD to 9 pM for the MBA, calculated as 3×SD/sensitivity, where SD is the standard deviation of the baseline current) was achieved due to the low noise currents generated by the microsensor. A thirty-fold increase in sensitivity (0.77 ± 0.02 A M^{-1} cm^{-2} for the MBA vs 0.023 ± 0.002 A M^{-1} cm^{-2} for the SPD) was accompanied by an enhancement of the reproducibility for measurements using 5 different bioelectrodes prepared in the same manner (2.5% RSD for the MBA vs 8.9% for the SPD) at the microscale enzyme-modified electrode due to the establishment of convergent diffusion. Moreover, an expansion of the dynamic range (0.2–110 μM for the MBA compared to 2–110 μM for the SPD) was observed with the decrease in sensor dimensions.

The MBA-based biosensors could be stored for one month in 0.1 M acetate buffer (pH 5.0) or for 2 weeks in dry state without observable loss of enzyme activity, but they are not applicable for long-term repeatable use after storage. On the second day of measurements the biosensors has lost 20% of the current response compared to the first day of measurements.

4.4. Real sample analysis

Due to the wide substrate specificities towards phenol substrates, mediated bioelectrocatalysis of laccases can be utilized as a versatile platform for the development of reagentless, *in situ* monitoring devices for the detection of phenols.

Direct amperometric measurements of catechol in unsupported tap water (i.e. without addition of buffer or electrolyte) was utilized as a model for a water quality monitoring platform. A two-electrode setup, with a laccase-modified electrode polarization of −0.4 V with respect to a platinum wire used as a pseudo-reference electrode was applied in order to simplify the analytical system.

Unlike the microscale MBA-based biosensor, the macroscale laccase-modified SPD showed a poor and unreliable response in unsupported tap water towards catechol (Fig. A.7), which illustrates the advantage of using the microscale electrode geometry characterized by convergent diffusion [49]. The microsensor showed fast responses towards catechol with a high signal-to-noise ratio (Fig. A.8A) characterized by a linear range from 0.2 to 10 μM (0.022–1.1 mg L^{-1}), a sensitivity of 1.35 ± 0.4 A M^{-1} cm^{-2} and a dynamic range up to 43 μM (4.7 mg L^{-1}) (Fig. A.8B). Tap water contamination by wastewater intrusion in a drinking water distribution network is an example of a failure that might occur and the detection of phenol as a marker of such a failure was investigated in a model study. First, the operational stability of the biosensor in tap water was investigated (Fig. A.8C). The biosensor demonstrated stable current response during 3 h. The small drift of the current response is possibly related to instability of the reference electrode rather than with the stability of the biosensor and can be overcome by optimization of the reference electrode. Amperometry at the laccase-based microsensor showed a reliable detection of 0.1% contamination by wastewater, illustrating the possibility of using the microsensor for tap water quality monitoring. (Fig. 4B).

The developed microscale sensor was also utilized for the analysis of laccase substrates in industrial samples of wastewater obtained from the water treatment facility at positions before and after different cleaning steps (Fig. 4A). The method of standard additions of catechol was utilized for the analysis of samples of low catechol equivalent concentrations (Fig. A.9A,B). For measurements in samples with concentrations outside the dynamic range of the microsensor, the current change recorded 20 s after a potential step of −0.4 V showed better stability and could be used as an analytical response (Fig. A.9C). The latter method was therefore used for all samples (Table A.2). Results obtained with the method of standard additions and by recording current transients showed good correlation for samples of low catechol equivalent concentrations (samples 2, 3 and 5). Table A.2 summarizes the measured concentrations of catechol equivalent for the different water samples. The large decrease of concentration of catechol equivalent illustrates the efficiency of the cleaning steps at the water treatment facility.

A correlation analysis was performed to compare the concentrations of catechol equivalent measured by the laccase-modified microsensor and the phenolic compounds assessed independently by GC–MS/MS (Fig. 4C). The concentrations of 2,6-di-tert-butyl-4-methylphenol, butyl-4-hydroxyanisol, 4-bromophenol, 2,4-dibromophenol, 2,4,6-tribromophenol, 4-tert-butylphenol, 4-iso-nonylphenol, pentachlorophenol, bisphenol A and triclosan were measured by GC–MS/MS with a mass-spectrometry library analysis. It is seen that the deviation is larger at lower concentrations, which illustrates the lower limits of detection achieved by GC–MS/MS. The correlation of catechol equivalent with the total concentration of phenolic compounds showed a good correlation for concentrations above the limit for phenols in wastewaters

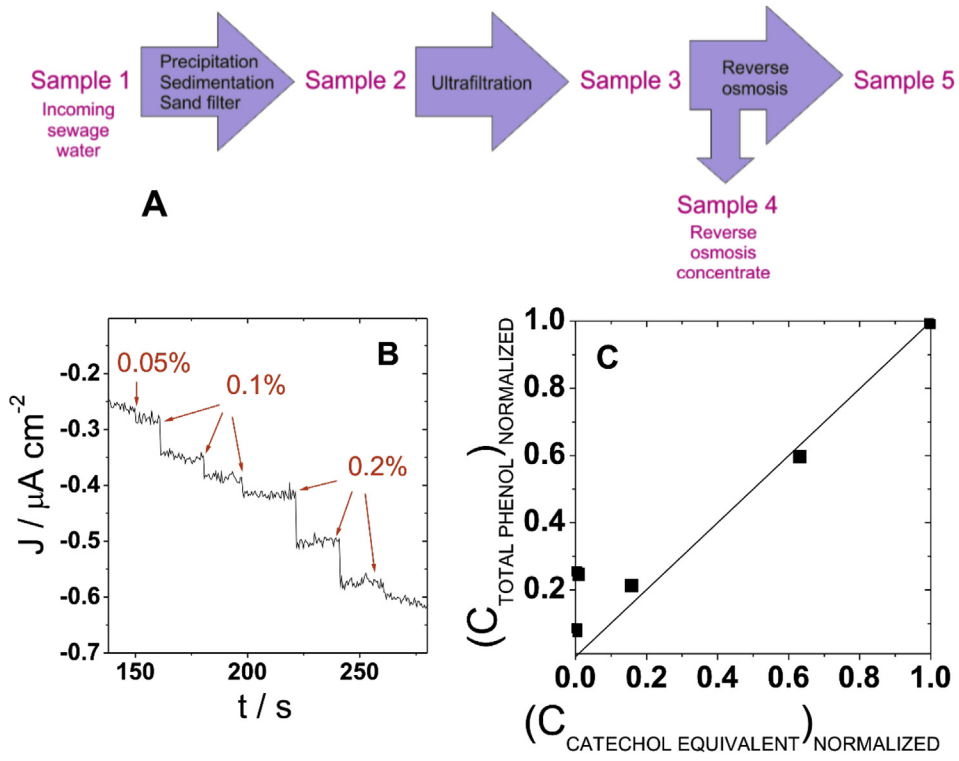

Fig. 4. Water analysis by the laccase-modified MBA. **A**: Scheme of water samples from different stages of wastewater cleaning; **B**: Amperometric response of the laccase-based microsensor to additions of sewage water (Sample 1) to tap water at −0.4 V vs Pt wire; **C**: Correlation analysis of catechol equivalent concentrations measured by the laccase-based microsensor with total phenol concentrations assessed by GC–MS/MS.

(0.1 mg L^{-1}) [4]. Thus, while also offering the advantages of continuous, *in situ* monitoring and low cost, the developed reagentless laccase-based microsensor showed a good correlation with the GC–MS/MS protocol.

5. Conclusions

A novel laccase based microsensor applicable for *in situ* monitoring of phenols in weakly supported media has been demonstrated for the first time. We showed by numerical simulations using the finite element method that the electrochemical behavior of the fabricated microband electrode is dominated by convergent diffusion. We showed a significant improvement of the analytical performance of a microband enzyme biosensor, compared to corresponding macroscale systems, due to the establishment of convergent diffusion in the microband case rather than the planar mass transfer for the macroscale systems. This enhanced laccase-based microsensor displayed potential to directly monitor tap water contamination by wastewater intrusion in a drinking water distribution network and revealed a correlation with a standard method for *in situ* monitoring of total phenols in wastewaters without additional sample preatretment.

Acknowledgments

The authors would like to thank The Swedish research council Formas (the grant number 245-2010-1062), the research centre Security Link (the grant VINNOVA 2009-00966) and the Norrköpings fond för Forskning och Utveckling for financial support and The Swedish National Infrastructure for Computing (SNIC) at Linköping University for simulation resources. The authors would like to thank VINNOVA and the VINNOVA funded project "Tomorrow's municipal wastewater - a production facility for utilities" for supplying sewage water samples from the sewage treatment pilot plant at Hammarby Sjöstad, Stockholm, Sweden and Mr. Mikael Remberger at the Swedish Environmental Research Institute (IVL) for performing the GC–MS/MS reference measurements of the phenolic compounds.

Appendix A. Supplementary data

Supplementary data related to this article can be found at http://dx.doi.org/10.1016/j.aca.2015.12.006.

References

[1] The United Nations, Managing Water under Uncertainty and Risk, 2012. World Water Development Report 4.
[2] A.I. Yaropolov, A.N. Kharybin, J. Emneus, G. Markovarga, L. Gorton, Flow-injection analysis of phenols at a graphite electrode modified with co-immobilized laccase and tyrosinase, Anal. Chim. Acta 308 (1995) 137–144.
[3] S.Y. Sheikheldin, T.J. Cardwell, R.W. Cattrall, M.D. Luque de Castro, S.D. Kolev, Determination of phenol in water by pervaporation–flow injection analysis, Anal. Chim. Acta 419 (2000) 9–16.
[4] T. Al-Khalid, M.H. El-Naas, Aerobic Biodegradation of Phenols: A Comprehensive Review, Crit. Rev. Environ. Sci. Technol. 42 (2012) 1631–1690.
[5] Commission of the European Communities, Council Directive 98/83/EC of 3 November 1998 on the quality of water intended for human consumption Official Journal L 330, 05/12/1998 P. 0032–0054.
[6] T.A. Larue, E.R. Blakley, Spectrophotometric determination of catechols with 4-aminoantipyrine, Anal. Chim. Acta 31 (1964) 400–403.
[7] A. Penalver, E. Pocurull, F. Borrull, R.M. Marce, Solid-phase microextraction coupled to high-performance liquid chromatography to determine phenolic compounds in water samples, J. Chromatogr. A 953 (2002) 79–87.
[8] P.A. Realini, Determination of priority pollutant phenols in water by HPLC, J. Chromatogr. Sci. 19 (1981) 124–129.
[9] F. Karim, A.N.M. Fakhruddin, Recent advances in the development of biosensor for phenol: a review, Rev. Environ. Sci. Bio-Technology 11 (2012) 261–274.
[10] B. Haghighi, L. Gorton, T. Ruzgas, L.J. Jonsson, Characterization of graphite

electrodes modified with laccase from Trametes versicolor and their use for bioelectrochemical monitoring of phenolic compounds in flow injection analysis, Anal. Chim. Acta 487 (2003) 3–14.
[11] R. Solna, P. Skladal, Amperometric flow-injection determination of phenolic compounds using a biosensor with immobilized laccase, peroxidase and tyrosinase, Electroanalysis 17 (2005) 2137–2146.
[12] H.P. Call, I. Mucke, History, overview and applications of mediated lignolytic systems, especially laccase-mediator-systems (Lignozym(R)-process), J. Biotechnol. 53 (1997) 163–202.
[13] D.W. Li, L. Luo, Z.Y. Pang, L. Ding, Q.Q. Wang, H.Z. Ke, F.L. Huang, Q.F. Wei, Novel Phenolic Biosensor Based on a Magnetic Polydopamine-Laccase-Nickel Nanoparticle Loaded Carbon Nanofiber Composite, Acs Appl. Mater. Interfaces 6 (2014) 5144–5151.
[14] X.H. Zhou, L.H. Liu, X. Bai, H.C. Shi, A reduced graphene oxide based biosensor for high-sensitive detection of phenols in water samples, Sensors Actuators B-Chemical 181 (2013) 661–667.
[15] D. Brondani, B. de Souza, B.S. Souza, A. Neves, I.C. Vieira, PEI-coated gold nanoparticles decorated with laccase: A new platform for direct electrochemistry of enzymes and biosensingapplications, Biosens. Bioelectron. 42 (2013) 242–247.
[16] M.L. Mena, V. Carralero, A. Gonzalez-Cortes, P. Yanez-Sedeno, J.M. Pingarron, Laccase biosensor based on N-succinimidyl-3-thiopropionate-functionalized gold electrodes, Electroanalysis 17 (2005) 2147–2155.
[17] S. Timur, N. Pazarlioglu, R. Pilloton, A. Telefoncu, Thick film sensors based on laccases from different sources immobilized in polyaniline matrix, Sensors Actuators B-Chemical 97 (2004) 132–136.
[18] R.G. Compton, G.G. Wildgoose, N.V. Rees, I. Streeter, R. Baron, Design, fabrication, characterisation and application of nanoelectrode arrays, Chem. Phys. Lett. 459 (2008) 1–17.
[19] S. Cosnier, Biomolecule immobilization on electrode surfaces by entrapment or attachment to electrochemically polymerized films. A review, Biosens. Bioelectron. 14 (1999) 443–456.
[20] R.S. Freire, N. Duran, L.T. Kubota, Effects of fungal laccase immobilization procedures for the development of a biosensor for phenol compounds, Talanta 54 (2001) 681–686.
[21] X.C. Li, H.J. Zhou, P. Yu, L. Su, T. Ohsaka, L.Q. Mao, A miniature glucose/O-2 biofuel cell with single-walled carbon nanotubes-modified carbon fiber microelectrodes as the substrate, Electrochem. Commun. 10 (2008) 851–854.
[22] K.R. Wehmeyer, M.R. Deakin, R.M. Wightman, Anal. Chem. 57 (1985) 1913.
[23] A.J. Bard, L.R. Faulkner, Electrochemical Methods. Fundamentals and Applications, 2 ed., John Wiley & Sons, Inc, 2001.
[24] X.J. Huang, A.M. O'Mahony, R.G. Compton, Microelectrode Arrays for Electrochemistry: Approaches to Fabrication, Small 5 (2009) 776–788.
[25] M.Y. Vagin, A.N. Sekretaryova, R.S. Reategui, I. Lundstrom, F. Winquist, M. Eriksson, Arrays of Screen-Printed Graphite Microband Electrodes as a Versatile Electroanalysis Platform, ChemElectroChem 1 (2014) 755–762.
[26] R.O. Kadara, N. Jenkinson, C.E. Banks, Screen printed recessed microelectrode arrays, Sensors Actuators B-Chemical 142 (2009) 342–346.
[27] A. Konash, A.R. Harris, J. Zhang, D. Elton, M. Hyland, G. Kennedy, A.M. Bond, Theoretical and experimental evaluation of screen-printed tubular carbon ink disposable sensor well electrodes by dc and Fourier transformed ac voltammetry, J. Solid State Electrochem. 13 (2009) 551–563.
[28] P.J. Welford, J. Freeman, S.J. Wilkins, J.D. Wadhawan, C.E.W. Hahn, R.G. Compton, Laminated microelectrodes: A simple approach to the construction of inexpensive microelectrodes with a variety of geometries, Anal. Chem. 73 (2001) 6088–6092.
[29] C. Amatore, J.M. Saveant, D. Tessier, Charge-transfer at partially blocked surfaces - a model for the case of microscopic active and inactive sites, J. Electroanal. Chem. 147 (1983) 39–51.
[30] M. Ardhaoui, M.H. Zheng, J. Pulpytel, D. Dowling, C. Jolivalt, F.A. Khonsari, Plasma functionalized carbon electrode for laccase-catalyzed oxygen reduction by direct electron transfer, Bioelectrochemistry 91 (2013) 52–61.
[31] C. Bourdillon, C. Demaille, J. Gueris, J. Moiroux, J.M. Saveant, A fully active monolayer enzyme electrode derivatized by antigen-antibody attachment, J. Am. Chem. Soc. 115 (1993) 12264–12269.
[32] B.A. Brookes, T.J. Davies, A.C. Fisher, R.G. Evans, S.J. Wilkins, K. Yunus, J.D. Wadhawan, R.G. Compton, Computational and experimental study of the cyclic voltammetry response of partially blocked electrodes. Part 1. Nonoverlapping, uniformly distributed blocking systems, J. Phys. Chem. B 107 (2003) 1616–1627.
[33] J. Wang, M. Pedrero, H. Sakslund, O. Hammerich, J. Pingarron, Electrochemical activation of screen-printed carbon strips, Analyst 121 (1996) 345–350.
[34] T. Nagaoka, T. Yoshino, Surface-properties of electrochemically pretreated glassy-carbon, Anal. Chem. 58 (1986) 1037–1042.
[35] C. Chollet, C. Chanseau, B. Brouillaud, M.C. Durrieu, RGD peptides grafting onto poly(ethylene terephthalate) with well controlled densities, Biomol. Eng. 24 (2007) 477–482.
[36] R.G. Compton, C.E. Banks, Understanding Voltammetry, World Scientific, 2007.
[37] C. Johannes, A. Majcherczyk, Laccase activity tests and laccase inhibitors, J. Biotechnol. 78 (2000) 193–199.
[38] D. Quan, W.S. Shin, Modification of electrode surface for covalent immobilization of laccase, Mater. Sci. Eng. C-Biomimetic Supramol. Syst. 24 (2004) 113–115.
[39] J. Cassidy, J. Ghoroghchian, F. Sarfarazi, J.J. Smith, S. Pons, Electrochim. Acta 31 (1986) 629.
[40] H. Reller, E. Kirowa-Eisner, E. Gileadi, J. Electroanal. Chem. 161 (1984) 247.
[41] R.J. Forster, T.E. Keyes, Behavior of Ultramicroelectrodes, Elsevier, Amsterdam, 2007.
[42] K. Wang, J. Tang, Z. Zhang, Y. Gao, G. Chen, Laccase on Black Pearl 2000 modified glassy carbon electrode: Characterization of direct electron transfer and biological sensing properties for pyrocatechol, Electrochimica Acta 70 (2012) 112–117.
[43] J. Cabaj, J. Sołoducho, A. Nowakowska-Oleksy, Langmuir–Blodgett film based biosensor for estimation of phenol derivatives, Sensors Actuators B Chem. 143 (2010) 508–515.
[44] X.-H. Zhou, L.-H. Liu, X. Bai, H.-C. Shi, A reduced graphene oxide based biosensor for high-sensitive detection of phenols in water samples, Sensors Actuators B Chem. 181 (2013) 661–667.
[45] R. Rawal, S. Chawla, C.S. Pundir, Polyphenol biosensor based on laccase immobilized onto silver nanoparticles/multiwalled carbon nanotube/polyaniline gold electrode, Anal. Biochem. 419 (2011) 196–204.
[46] Y.Y. Zhou, L. Tang, G.M. Zeng, J. Chen, Y. Cai, Y. Zhang, G.D. Yang, Y.Y. Liu, C. Zhang, W.W. Tang, Mesoporous carbon nitride based biosensor for highly sensitive and selective analysis of phenol and catechol in compost bioremediation, Biosens. Bioelectron. 61 (2014) 519–525.
[47] G.E. Cabaniss, A.A. Diamantis, W.R. Murphy, R.W. Linton, T.J. Meyer, Electrocatalysis of proton-coupled electron-transfer reactions at glassy-carbon electrodes, J. Am. Chem. Soc. 107 (1985) 1845–1853.
[48] L. Gorton, A. Lindgren, T. Larsson, F.D. Munteanu, T. Ruzgas, I. Gazaryan, Direct electron transfer between heme-containing enzymes and electrodes as basis for third generation biosensors, Anal. Chim. Acta 400 (1999) 91–108.
[49] R.G. Compton, G.G. Wildgoose, N.V. Reese, I. Streeter, R. Baron, Chem. Phys. Lett. 459 (2008) 1.